Journal of Sound and Vibration (1997) **199**(2), 237–251

STEADY-STATE RESPONSE OF THE FLEXIBLE CONNECTING ROD OF A SLIDER-CRANK MECHANISM WITH TIME-DEPENDENT BOUNDARY CONDITION

R.-F. FUNG AND H.-H. CHEN

Department of Mechanical Engineering, *Chung Yuan Christian University*, *Chung-Li*, *Taiwan* 32023, *Republic of China*

(*Received* 29 *May* 1995, *and in final form* 15 *April* 1996)

This paper presents a finite element method for the dynamic analysis of a flexible connecting rod in a slider-crank mechanism with time-dependent boundary conditions. Kinetic and strain energies of the flexible link are formulated and used with Hamilton's principle to develop the governing equations. Time-dependent boundary conditions instead of simply-supported end conditions are used to define the displacement field of the connecting rod. A special finite element method is developed for such a time-dependent boundary condition. The equations of motion are transformed into a set of ordinary differential equations and the harmonic balance method is used to obtain the steady-state amplitudes and rotary angles. The results are compared for the time-dependent and simply-supported end conditions.

1. INTRODUCTION

Dynamic analysis of a flexible connecting rod of a slider-crank mechanism has become the subject of many investigations, which include transient, steady-state and dynamic stability analyses. The steady-state solutions and the elastic stability for both the transverse and longitudinal vibrations of the elastic connecting rod in a high-speed slider-crank mechanism were obtained by Jasinski *et al*. [1]. The response of the system was found by Viscomi and Ayre [2] to be dependent upon five parameters; length, mass, damping, link frequency and external piston force. Sadler and Sandor [3] developed a method of kinetoelastodynamic analysis. They employed lumped parameter models to simulate the moving mechanism components. The transient responses in both transverse and longitudinal directions were investigated by Chu and Pan [4] on the basis of the ratios between the length of the crank and the length of the connecting rod, rotating speeds of the crank, viscous damping, and the natural frequencies.

Badlni and Midha [5] investigated dynamic stability by using Euler-Bernoulli and Timoshenko beam theories. Badlni and Midha [6] investigated the dynamic behavior of an initially curved connecting rod. Zue and Chen [7] studied the dynamic stability of a connecting rod based on a perturbation technique, in which the ratio between crank radius and rod length was assumed to be small. Tadjbakhsh [8] studied the stability of the slider-crank mechanism with no restriction on the nature of the response and without simplifying geometric assumptions. Hsieh and Shaw [9] investigated the dynamic behavior and determined the manner in which this response depended on the system parameters with

0022–460X/97/020237 + 15 $25.00/0/sv960612

particular emphasis on non-linear analyses of the dynamic response near resonance conditions.

The above references assume simply-supported boundary conditions at both ends of the connecting rod, i.e., the moment and displacement vanish at both ends. Agrawal and Shabana [10] presented the comparisons between the results obtained using different sets of boundary conditions, and discussed the relationship between the boundary conditions and the co-ordinate system of the flexible links. In this paper, Hamilton's principle and the finite element method are applied to formulate the governing equation of a flexible rod. The effect of time-dependent boundary condition on the steady-state response is the main subject in this paper. The harmonic balance method is applied to obtain the steady-state amplitudes and rotary angles. These results are compared with those obtained by assuming the simply-supported boundary conditions for the connecting rod. It is found that the steady-state transverse responses of the present work are near those of the simple support, but the responses in the axial direction are considerably different and the natural frequency decreases.

2. FORMULATION OF GOVERNING EQUATION

The slider-crank mechanism shown in Figure 1a consists of the crank OA with length r, the flexible prismatic rod AB with length L, and the slider B of mass M_4. Other symbols in this figure are as follows: N and F are the normal and the tangential forces acting on the piston, θ is the crank angle, and ϕ is the angle between the X-axis and the undeformed axis of the connecting rod. Observe that ϕ is defined positive clockwise and is measured

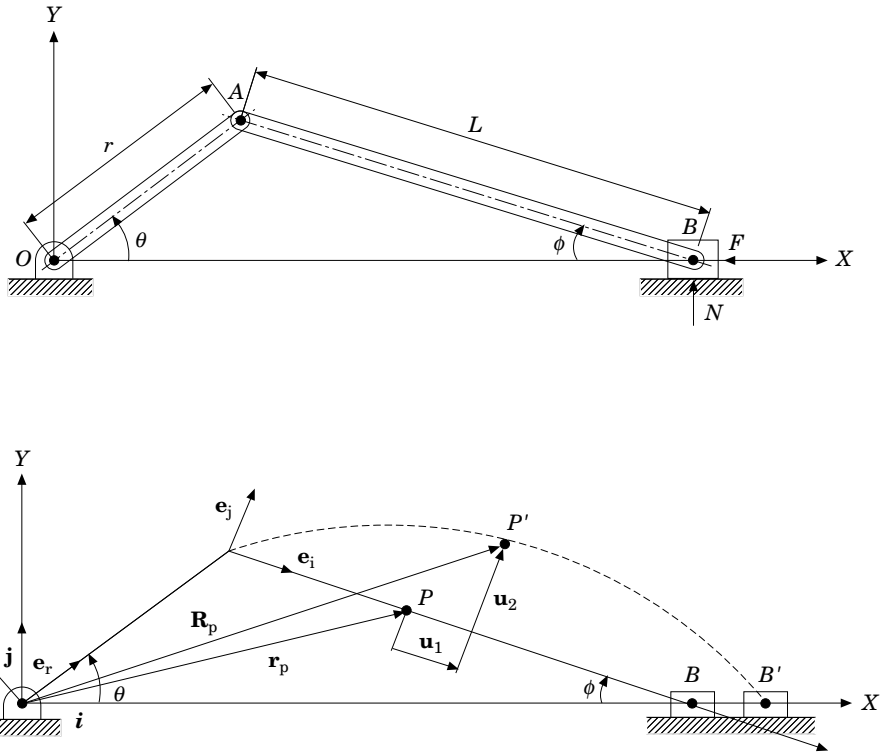

Figure 1. Slider-crank mechanism with a flexible connecting rod. (a) Undeformed configuration. (b) Deformed configuration.

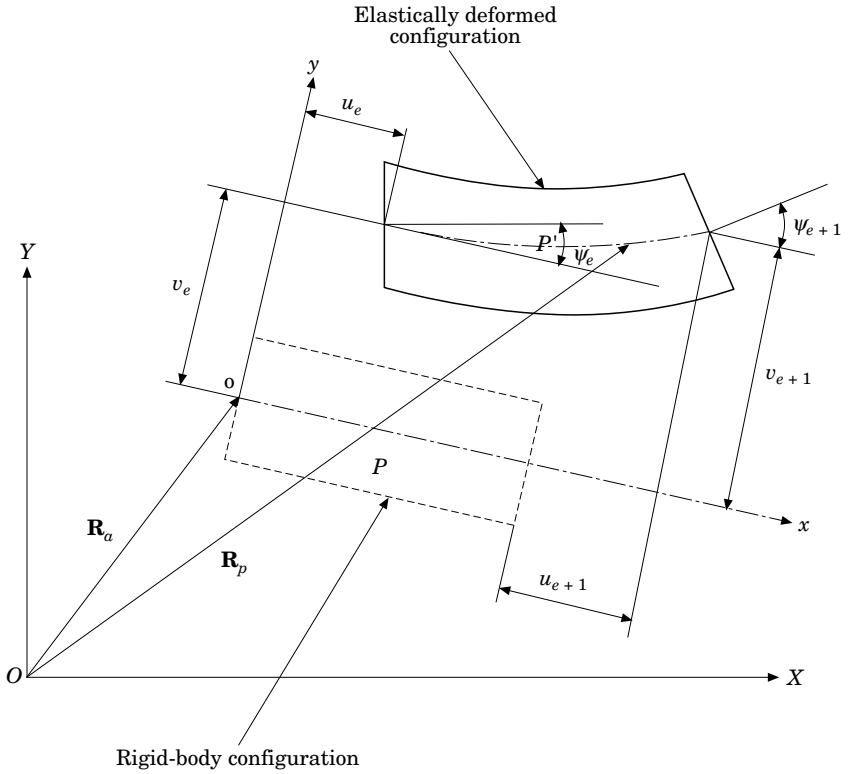

Figure 2. A beam element undergoing gross motion and elastic deformation.

from the negative X-axis. Figure 1b shows the deformed slider-crank mechanism. Since the slider moves along the X-axis, point B, connecting the connecting rod and the slider, also moves along the X-axis.

The flexible connecting rod is modeled as a Timoshenko beam and Hamilton's principle is used to derive the equation of motion of the rod. The following assumptions are made in the derivation of the equation of motion: (a) The crank is rigid, (b) the cross-sectional area A, the modulus of elasticity E, the second moment of area I, and the mass density ρ of the connecting rod are constant, and (c) the applied force and the friction force acting on the slider are negligible.

2.1. FLEXIBLE DEFORMATION CONSTRAINT

The deformed slider-crank mechanism is shown in Figure 1(b). $(\mathbf{i}, \mathbf{j})$ are unit vectors of the fixed co-ordinate system (OXY), $(\mathbf{e}_r, \mathbf{e}_\theta)$ and $(\mathbf{e}_i, \mathbf{e}_j)$ are unit vectors of the moving co-ordinates originating at O and A respectively. The displacement field is

$$u_1(x, y, t) = u(x, t) - y\psi(x, t), \qquad u_2(x, y, t) = v(x, t), \tag{1a, b}$$

where u and v represent the axial and transverse displacements of the connecting rod respectively, and ψ is the slope of the deflection curve due to bending deformation only. The beam element undergoes gross motion and elastic deformation (Figure 2). The position vector of arbitrary point P of the connecting rod with respect to the fixed frame is

$$\mathbf{R}_P = r\mathbf{e}_r + x_o\mathbf{e}_i + (x + u_1)\mathbf{e}_i + (y + u_2)\mathbf{e}_j = r\mathbf{e}_r + (x_o + x + u - y\psi)\mathbf{e}_i + (y + v)\mathbf{e}_j,$$

where x_o is the distance measured from point A to the original point o of the local co-ordinate, (x, y) is the position of point P measured from the local original point o of the particular element concerned.

When the slider moves along the X-axis, the pin joint B, connecting the connecting rod and the slider, also moves along X-axis. Thus, the condition of point B denotes that the displacement in the Y-direction is zero, so that

$$0 = \mathbf{R}_B \cdot \mathbf{j} = r \sin\theta - [L + u_{n+1}] \sin\phi + v_{n+1} \cos\phi,$$

where n is the element number of the connecting rod, and u_{n+1} and v_{v+1} are the axial and transverse displacements at point B respectively. Substituting the geometric relation of a rigid body

$$r \sin\theta = L \sin\phi \tag{2}$$

into the above equation, one obtains

$$v_{n+1} = u_{n+1} \tan\phi, \tag{3}$$

which is the flexible deformation constraint of the last node of the connecting rod at point B. Equation (3) was also obtained by Hsieh and Shaw [9]; however, they approximated $v_{n+1} = 0$ in the non-linear analysis. Equation (3) is the time-dependent boundary condition and it is the same as Fahrang and Midha [11].

It is seen that $u_{n+1} = v_{n+1} = 0$ for the assumption of a simply-supported end is also included in equation (3). The investigators [7, 8] assumed that the right end of the connecting rod was simply supported and obtained zero transverse displacement at point B. In the present work, u_{n+1} and v_{n+1} might not be zeros at point B. In case of the assumption of zero transverse displacement at end point B, $v_{n+1} = 0$, one then has $u_{n+1} = 0$ from (3). It should be noted that the case with $u_{n+1} = v_{n+1} = 0$, where there is no deformation at end point B, the end position of elastic assumption of the connecting rod will be the same as that of rigid body assumption.

However, in the present work the end point B of the connecting rod moves along the X-axis, both u_{n+1} and v_{n+1} are not independent, and are related by (3). Therefore, the piston position could be predicted due to the elastic deformation. With the help of Figure 3, it is convenient to define the horizontal displacement at point B as

$$D_B = u_{n+1}/\cos\phi. \tag{4}$$

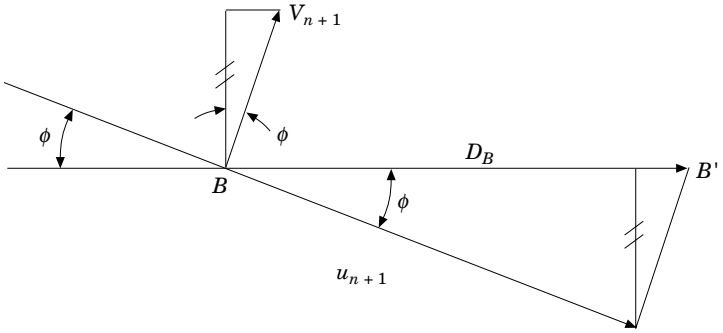

Figure 3. At end point B, the displacement relationship between D_B, u_{n+1} and v_{n+1}.

2.2. KINETIC AND STRAIN ENERGIES

Differentiating equation (2) with respect to time, the absolute velocity of arbitrary point P on an element of the connecting rod can be written as

$$\begin{aligned}\dot{\mathbf{R}}_P &= r\dot{\theta}\mathbf{e_0} + (u_t - y\psi_t)\mathbf{e_i} + v_t\mathbf{e_j} - \dot{\phi}\mathbf{e_k} \times [(x_o + x + u - y\psi)\mathbf{e_i} + (y + v)\mathbf{e_j}\\ &= [-r\dot{\theta}\sin(\theta + \phi) + u_t - y\psi_t + \dot{\phi}(y + v)]\mathbf{e_i} + [r\dot{\theta}\cos(\theta + \phi) + v_t\\ &\quad - \dot{\phi}(x_o + x + u - y\psi)]\mathbf{e_j}.\end{aligned}$$

In this paper, the connecting rod is discretized into n elements of equal length l. The kinetic energy of the connecting rod can be expressed as

$$T_3 = \tfrac{1}{2}\int_V \rho\dot{\mathbf{R}}_P(x, y, t)\cdot\dot{\mathbf{R}}_P(x, y, t)\,\mathrm{d}V = \sum_{e=1}^{n} T_e, \tag{5}$$

where

$$\begin{aligned}T_e = \tfrac{1}{2}\int_0^l (\rho A\{[-r\dot{\theta}\sin(\theta + \phi)u_t + v\dot{\phi}]^2\\ +[r\dot{\theta}\cos(\theta + \phi) + v_t - \dot{\phi}(x_o + x + u)]^2\} + \rho I/2[(\dot{\phi} - \psi_t)^2 + \dot{\phi}^2\psi^2])\,\mathrm{d}x,\end{aligned} \tag{6}$$

is the kinetic energy of an element.

The linear Lagrangian strains are

$$\epsilon_{xx} = u_x - y\psi_x, \quad \epsilon_{yy} = 0, \quad \epsilon_{xy} = \tfrac{1}{2}(v_x - \psi), \tag{7}$$

where the higher order terms $\frac{1}{2}v_x^2$, $u_x\psi$, $y\psi\psi_x$ are neglected in ϵ_{xx} and ϵ_{xy}. The strain energy of the connecting rod can be expressed as

$$U_3 = \tfrac{1}{2}\int_V \sigma_{ij}\epsilon_{ij}\,\mathrm{d}V = \sum_{e=1}^{n} U_e, \tag{8}$$

where

$$U_e = \tfrac{1}{2}\int_0^l [EAu_x^2 + kGA(v_x - \psi)^2 + EI\psi_x^2]\,\mathrm{d}x, \tag{9}$$

is the strain energy of an element.

The kinetic energy of the crank is

$$T_2 = \tfrac{1}{2}M_2(r/2\theta_t)^2 + \tfrac{1}{2}J_{2c}\theta_t^2 = \tfrac{1}{8}M_2r^2\theta_t^2 + \tfrac{1}{2}J_{2c}\theta_t^2, \tag{10}$$

where M_2 is the crank mass and J_{2c} is its mass momentum of inertia. Note that the variation of crank kinetic energy is zero since θ_t is prescribed.

The kinetic energy of the slider is

$$T_4 = \tfrac{1}{2}M_4\dot{\mathbf{R}}_B\cdot\dot{\mathbf{R}}_B, \tag{11}$$

where

$$\dot{\mathbf{R}}_B = [-r\theta_t\sin(\theta + \phi) + u_t + v\phi_t]\mathbf{e_i} + [r\theta_t\cos(\theta + \phi) - (L + u)\phi_t + v_t]\mathbf{e_j}.$$

The work done by the applied force F and the friction force N acting at the slider is

$$W = [(F - \mu N)\mathbf{i} + N\mathbf{j}]\cdot\mathbf{R}_B. \tag{12}$$

2.3. FINITE ELEMENT FORMULATION

The usual approach of the finite element method is to assume each unknown deformation to be approximated by a finite series. The deflection v of the beam element can be described by using a cubic polynomial as

$$v = a_0 + a_1 x + a_2 x^2 + a_3 x^3,$$

and the deflection u of the beam element by using a polynomial as

$$u = c_0 + c_1 x,$$

where $a_0 \sim a_3$ and $c_0 \sim c_1$ are the generalized co-ordinates.

On non-dimensionalization by substituting $\xi = x/l$, the element deflections u, v and rotation ψ can be expressed in terms of the nodal displacement vector $\{\mathbf{q}\}_e$ as $\{u_e, v_e, \psi_e, u_{e+1}, v_{e+1}, \psi_{e+1}\}^{\mathrm{T}}$. Sequentially

$$\begin{Bmatrix} u \\ v \\ \psi \end{Bmatrix} = \begin{bmatrix} N_{u_1} & 0 & 0 & N_{u_2} & 0 & 0 \\ 0 & N_{v_1} & N_{v_2} & 0 & N_{v_3} & N_{v_4} \\ 0 & N_{\psi_1} & N_{\psi_2} & 0 & N_{\psi_3} & N_{\psi_4} \end{bmatrix} \begin{Bmatrix} u_i \\ v_i \\ \psi_i \\ u_j \\ v_j \\ \psi_j \end{Bmatrix}. \tag{13}$$

The shape functions about u, v and ψ are detailed in Appendix A.

Substituting equation (13) into equation (6) and expressing it in terms of the nodal displacement vector $\{\mathbf{q}\}_e$, one obtains the kinetic energy as follows

$$T_e = \tfrac{1}{2}\{\dot{\mathbf{q}}\}_e^{\mathrm{T}}[m_1]\{\dot{\mathbf{q}}\}_e + \tfrac{1}{2}\{\dot{\mathbf{q}}\}_e^{\mathrm{T}}[m_2]\{\mathbf{q}\}_e + \{\mathbf{q}\}_e^{\mathrm{T}}[m_c]\{\dot{\mathbf{q}}\}_e + [m_{qt}]\{\dot{\mathbf{q}}\}_e + [m_q]\{\mathbf{q}\}_e + X_1, \tag{14}$$

where $[m_1]$, $[m_2]$, $[m_c]$ $[m_{qt}]$, $[m_q]$ and X_1 are detailed in Appendix A.

The derivatives of u and v with respect to x, the curvature K and the shear strain γ within the element can be written, respectively, as

$$u_x = \mathrm{d}u/\mathrm{d}x = [B_u]\{\mathbf{q}\}_e, \quad v_x = \mathrm{d}v/\mathrm{d}x = [B_v]\{\mathbf{q}\}_e, \tag{15a, b}$$

$$K = \mathrm{d}\psi/\mathrm{d}x = [B_b]\{\mathbf{q}\}_e, \quad \gamma = \mathrm{d}v/\mathrm{d}x - \psi = [B_s]\{\mathbf{q}\}_e, \tag{15c, d}$$

where

$$[B_u] = \mathrm{d}/\mathrm{d}x[N_u], \quad [B_v] = \mathrm{d}/\mathrm{d}x[N_\psi], \quad [B_b] = \mathrm{d}/\mathrm{d}x[N_v], \quad [B_s] = \mathrm{d}/\mathrm{d}x[N_u] - [N_\psi]. \tag{16a–d}$$

The strain energy of one element, equation (9), can be expressed as

$$U_e = \tfrac{1}{2}\{\mathbf{q}\}_e^{\mathrm{T}}[K_u]\{\mathbf{q}\}_e + \tfrac{1}{2}\{\mathbf{q}\}_e^{\mathrm{T}}[K_s]\{\mathbf{q}\}_e + \tfrac{1}{2}\{\mathbf{q}\}_e^{\mathrm{T}}[K_b]\{\mathbf{q}\}_e, \tag{17}$$

where $[K_u]$, $[K_b]$ and $[K_s]$ can be seen in Appendix A.

The kinetic energy of the slider, equation (11), can be expressed as

$$T_4 = \tfrac{1}{2}\{\dot{\mathbf{q}}\}_e^{\mathrm{T}}[m_{41}]\{\dot{\mathbf{q}}\}_e + \tfrac{1}{2}\{\mathbf{q}\}_e^{\mathrm{T}}[m_{42}]\{\mathbf{q}\}_e + \{\dot{\mathbf{q}}\}_e^{\mathrm{T}}[m_{43}]\{\mathbf{q}\}_e + \{\mathbf{q}\}_e^{\mathrm{T}}[m_{44}] + \{\dot{\mathbf{q}}\}_e^{\mathrm{T}}[m_{45}] + X_2, \tag{18}$$

where $[m_{41}]$, $[m_{42}]$, $[m_{43}]$, $[m_{44}]$, $[m_{45}]$, and X_2 are detailed in Appendix A. The work done by the force and friction force acting at the slider, equation (12), can be expressed as

$$W = \{\dot{\mathbf{q}}\}_n^{\mathrm{T}}[m_w] + X_3, \tag{19}$$

where $[m_w]$ and X_3 are detailed in Appendix A.

By using Hamilton's principle, one obtains

$$0 = \int_{t_1}^{t_2} \{\delta T_2 + \delta T_3 - \delta U_3 + \delta T_4 + \delta W\}\, \mathrm{d}t. \tag{20}$$

The variation of the crank kinetic energy δT_2 is zero, since θ_t is prescribed. The variation of the Lagrangian density of the connecting rod, the variation of the kinetic energy of the slider, and the virtual work done by the force and friction force acting at the slider are respectively

$$\int_{t_1}^{t_2} (\delta T_3 - \delta U_3)\, \mathrm{d}t = \int_{t_1}^{t_2} \sum_{e=1}^{n} \delta\{\mathbf{q}\}_e^{\mathrm{T}} \left(\frac{\partial L_e}{\partial \{\mathbf{q}\}_e} - \frac{\mathrm{d}}{\mathrm{d}t} \frac{\partial L_e}{\partial \{\dot{\mathbf{q}}\}_e} \right) \mathrm{d}t + \left[\sum_{e=1}^{n} \delta\{\mathbf{q}\}_e^{\mathrm{T}} \frac{\partial L_e}{\partial \{\dot{\mathbf{q}}\}_e} \right]_{t_1}^{t_2}, \tag{21a}$$

$$\int_{t_1}^{t_2} \delta T_4\, \mathrm{d}t = \int_{t_1}^{t_2} \delta\{\mathbf{q}\}_n^{\mathrm{T}} \left(\frac{\partial T_4}{\partial \{\mathbf{q}\}_n} - \frac{\mathrm{d}}{\mathrm{d}t} \frac{\partial T_4}{\partial \{\dot{\mathbf{q}}\}_n} \right) \mathrm{d}t + \left[\delta\{\mathbf{q}\}_n^{\mathrm{T}} \frac{\partial T_4}{\partial \{\dot{\mathbf{q}}\}_n} \right]_{t_1}^{t_2}, \tag{21b}$$

$$\int_{t_1}^{t_2} \delta W\, \mathrm{d}t = \int_{t_1}^{t_2} \delta\{\mathbf{q}\}_n^{\mathrm{T}} \frac{\partial W}{\partial \{\mathbf{q}\}_n}\, \mathrm{d}t. \tag{21c}$$

On substituting equations (21a–c) into equation (20),

$$0 = \int_{t_1}^{t_2} \left[\sum_{e=1}^{n-1} \delta\{\mathbf{q}\}_e^{\mathrm{T}} \left(\frac{\partial L_e}{\partial \{\mathbf{q}\}_e} - \frac{\mathrm{d}}{\mathrm{d}t} \frac{\partial L_e}{\partial \{\dot{\mathbf{q}}\}_e} \right) + \delta\{\mathbf{q}\}_n^{\mathrm{T}} \left(\frac{\partial L_n}{\partial \{\mathbf{q}\}_n} - \frac{\mathrm{d}}{\mathrm{d}t} \frac{\partial L_n}{\partial \{\dot{\mathbf{q}}\}_n} + \frac{\partial T_4}{\partial \{\mathbf{q}\}_n} \right.\right.$$

$$\left.\left. - \frac{\mathrm{d}}{\mathrm{d}t} \frac{\partial T_4}{\partial \{\dot{\mathbf{q}}\}_n} + \frac{\partial W}{\partial \{\mathbf{q}\}_n} \right) \right] \mathrm{d}t + \left[\sum_{e=1}^{n} \delta\{\mathbf{q}\}_e^{\mathrm{T}} \frac{\partial L_e}{\partial \{\dot{\mathbf{q}}\}_e} \right]_{t_1}^{t_2} + \left[\delta\{\mathbf{q}\}_n^{\mathrm{T}} \frac{\partial T_4}{\partial \{\dot{\mathbf{q}}\}_n} \right]_{t_1}^{t_2}, \tag{22}$$

where $L_e = T_e - U_e$ is the Lagrangian function of an element and $\{\mathbf{q}\}_e = \{u_e, v_e, \psi_e, u_{e+1}, v_{e+1}, \psi_{e+1}\}^{\mathrm{T}}$, n is the total number of the elements of the connecting rod. The varied path coincides with the true path at the two timing ends t_1 and t_2. It follows that $\delta q_e(x, t_1) = \delta q_e(x, t_2) = \delta q_n(x, t_1) = \delta q_n = (x, t_2) = 0$.

By using the finite element technique, assembling the equation of motion of the elements, the ordinary differential equation of the system can be expressed as

$$[\mathbf{M}]\{\ddot{\mathbf{Q}}\} + [\mathbf{C}]\{\dot{\mathbf{Q}}\} + [\mathbf{K}]\{\mathbf{Q}\} = [\mathbf{F}], \tag{23}$$

where

$$\{\mathbf{Q}\} = \{u_1, v_1, \psi_1, u_2, v_2, \psi_2, \ldots, u_{n+1}, v_{n+1}, \psi_{n+1}\}^{\mathrm{T}},$$

[**M**] and [**K**] are the global mass and stiffness matrices respectively, [**C**] is the global damping term, and [**F**] is the force term. The definitions of [**M**], [**K**], [**C**] and [**F**] are shown in Appendix A.

2.4. TIME-DEPENDENT BOUNDARY CONDITIONS

The flexible deformation constraint (3) is the relation of u_{n+1} and v_{n+1} at the last node. The condition must be added to the corresponding entries of the system matrix.

Point A is the common point of the rigid crank and the flexible connecting rod. Thus, the values $u_1 = 0$ and $v_1 = 0$ are specified. The slope angles ψ at points A and B are not

specified, therefore ψ_1 and ψ_{n+1} are free to rotate. With the boundary conditions $u_1 = v_1 = 0$, the first and the second rows and columns of the matrices [**M**], [**C**], [**K**] and the vector [**F**] will have to be eliminated.

Since the flexible deformation constraint (3) holds for any time, its time derivative relationships

$$\dot{v}_{n+1} = \dot{u}_{n+1} \tan \phi + u_{n+1} \dot{\phi} \sec^2 \phi, \tag{24a}$$

$$\ddot{v}_{n+1} = \ddot{u}_{n+1} \tan \phi + (2\dot{u}_{n+1}\dot{\phi} + u_{n+1}\ddot{\phi} + 2u_{n+1}\dot{\phi}^2 \tan \phi) \sec^2 \phi, \tag{24b}$$

also hold. Equations (24a, b) show the coupling relationship between the x- and y-directions at the last node point. Finally, two dependent equations are obtained which are introduced into the corresponding components of matrices [**M**], [**C**] and [**K**].

2.5. RAYLEIGH DAMPING

For most structures, the exact form of the damping matrix is unknown since the sources of energy loss are complicated. Also, in most cases, the effect of damping on the vibration mode shape of the structure is small.

It is possible to introduce Rayleigh damping into the differential equation of motion and can be written as in reference [12]

$$[\mathbf{R}_g] = \alpha[\mathbf{M}] + \beta[\mathbf{K}],$$

where $[\mathbf{R}_g]$ is the Rayleigh damping matrix and α and β are the mass and stiffness damping coefficients respectively. Rayleigh's damping is added to the [**C**] matrix of equation (23), which absorbs amplitudes of the high frequency modes.

3. STEADY-STATE ANALYSIS OF TIME-VARYING SYSTEM

In this paper, the non-dimensional length ratio is defined as $\lambda = r/L$, where L is the length of the connecting rod, and r is the length of the crank. For a small crank ($\lambda \ll 1$), all coefficient matrices of equation (23) can be simplified by applying a binomial expansion. Now, ϕ, $\dot{\phi}$, $\dot{\phi}^2$, $\ddot{\phi}$, $\sin(\theta + \phi)$, $\cos(\theta + \phi)$, $\sin \phi$, $\cos \phi$ and $\tan \phi$ are given as functions of θ and λ, and the details can be seen in Appendix B. Substituting them into the element matrices and retaining the terms up to $O(\lambda)$, the equation of motion of an element can be expressed as

$$[\mathbf{M}_A]_e\{\ddot{\mathbf{q}}\}_e + \lambda \cos \Omega t[\mathbf{C}_B]_e\{\dot{\mathbf{q}}\}_e + ([\mathbf{K}_A]_e + \lambda \sin \Omega t[\mathbf{K}_B]_e)\{\mathbf{q}\}_e = \lambda[\mathbf{F}_1]_e \cos \Omega t + \lambda[\mathbf{F}_2]_e \sin \mathbf{\Omega} t, \tag{25}$$

where $[\mathbf{M}_A]_e$, $[\mathbf{C}_B]_e$, $[\mathbf{K}_A]_e$, $[\mathbf{K}_B]_e$, $[\mathbf{F}_1]_e$ and $[\mathbf{F}_2]_e$ are detailed in Appendix A. It should be noted that $[\mathbf{M}_i]$, $[\mathbf{C}_i]$, $[\mathbf{K}_i]$ and $[\mathbf{F}_i]$ are all constant coefficient matrices and Ω is equal to the crank angular velocity $\dot{\theta}$.

Now the constraints (equations 3, 24a, b) of position, velocity, and acceleration can be expressed respectively as

$$v_{n+1} = \lambda u_{n+1} \sin \Omega t, \qquad \dot{v}_{n+1} = \lambda \dot{u}_{n+1} \sin \Omega t + \lambda \Omega u_{n+1} \cos \Omega t, \tag{26a, b}$$

$$\ddot{v}_{n+1} = \lambda \ddot{u}_{n+1} \sin \Omega t + 2\lambda \Omega \dot{u}_{n+1} \cos \Omega t - \lambda \Omega^2 u_{n+1} \sin \Omega t. \tag{26c}$$

Assembling equation (25) and considering the boundary conditions and geometric constraints, the equation of motion of the system can be simplified to

$$([\mathbf{M}_A] + \lambda \cos \Omega t[\mathbf{M}_a])\{\ddot{\mathbf{Q}}\} + \lambda \cos \Omega t([\mathbf{C}_B] + 2\Omega[\mathbf{M}_a])\{\dot{\mathbf{Q}}\} + ([\mathbf{K}_A] + \lambda \sin \Omega t([\mathbf{K}_B] + [\mathbf{K}_a] - \Omega^2[\mathbf{M}_a]))\{\mathbf{Q}\} = \lambda[\mathbf{F}_1] \cos \Omega t + \lambda[\mathbf{F}_2] \sin \Omega t. \tag{27}$$

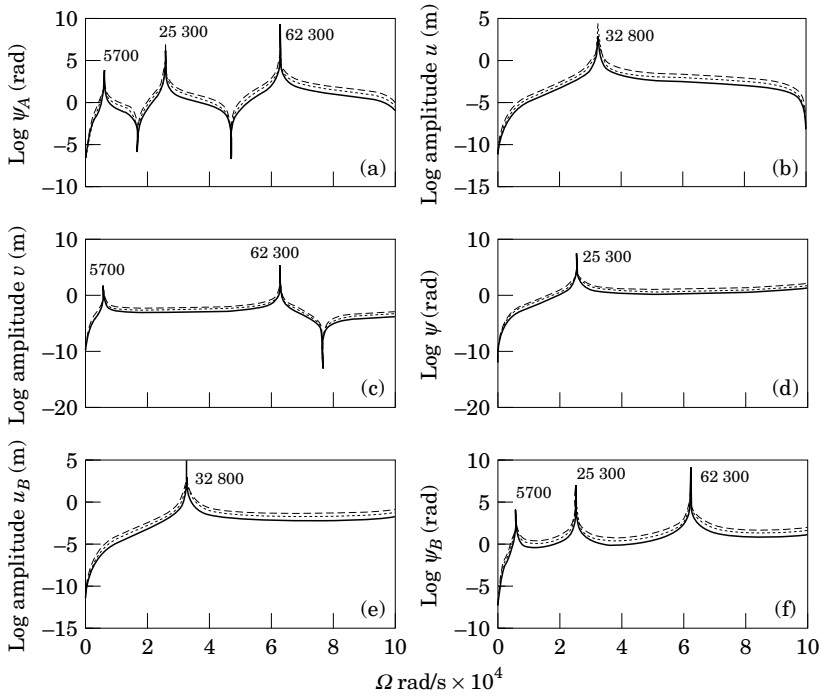

Figure 4. Steady-state responses versus crank angular velocity Ω. ——, $\lambda = 0{\cdot}2$; · · ·, $\lambda = 0{\cdot}35$; - - -, $\lambda = 0{\cdot}5$. (a) Log ψ_A; (b) Log $(A_p)u$; (c) Log $(A_p)v$; (d) Log ψ; (e) Log $(A_p)u_B$; (f) Log ψ_B.

where the $(3n+1)$th column of the $[\mathbf{M}_a]$ matrix is equal to the $(3n+2)$th column of the $[\mathbf{M}_A]$ matrix; the other column's elements in $[\mathbf{M}_a]$ are zeros. $[\mathbf{K}_a]$ is the same as the condition of the $[\mathbf{M}_a]$ matrix.

With constant angular velocity Ω of the crank, equation (27) is a second order time-varying periodic differential equation. The steady-state solutions of the linear parametric equation (27) can be determined by the harmonic balance method and the approximate solution with period $(T = 2\pi/\Omega)$ can be expressed in a Fourier series as

$$\{\mathbf{Q}\} = \{b_0\} + \sum_{k=2,4,6,\ldots}^{\infty} \{a_k\} \sin\frac{k\Omega t}{2} + \{b_k\} \cos\frac{k\Omega t}{2}. \tag{28}$$

Substituting equation (28) into equation (27) and comparing coefficients in the same harmonic term, one obtains a non-homogeneous algebraic equation in terms of $\{a_k\}$ and $\{b_k\}$ as

$$[\mathbf{K}_A]\{b_0\} + ((\lambda\Omega/2)[\mathbf{C}_B] + (\lambda/2)[\mathbf{K}_B] + (\lambda/2)[\mathbf{K}_a])\{a_2\} = \{0\}, \tag{29a}$$

$$(-\Omega^2[\mathbf{M}_A] + [\mathbf{K}_A])\{b_2\} + \lambda(\Omega[\mathbf{C}_B] + (1/2)[\mathbf{K}_B] + (1/2)[\mathbf{K}_a] - (\Omega^2/2)[\mathbf{M}_a])\{a_4\} = \lambda[\mathbf{F}_1], \tag{29b}$$

$$\lambda([\mathbf{K}_B] + [\mathbf{K}_a] - \Omega^2[\mathbf{M}_a])\{b_0\} + (-\Omega^2[\mathbf{M}_A] + [\mathbf{K}_A])\{a_2\} + ((\lambda\Omega^2/2)[\mathbf{M}_a] - \lambda\Omega[\mathbf{C}_B] - (\lambda/2)[\mathbf{K}_B] - (\lambda/2)[\mathbf{K}_a])\{b_4\} = \lambda[\mathbf{F}_2], \tag{29c}$$

$$(-(r^2\Omega^2/4)[\mathbf{M}_A] + [\mathbf{K}_A])\{a_r\} + (-(\lambda(r-2)^2\Omega^2/8)[\mathbf{M}_a] - (\lambda(r-2)\Omega/4)([\mathbf{C}_B] + 2\Omega[\mathbf{M}_a]) + 2\Omega(\mathbf{M}_a]) + (\lambda/2)([\mathbf{K}_B] + [\mathbf{K}_a] - \Omega^2[\mathbf{M}_a]))\{b_{r-2}\} + ((\lambda(r+2)^2\Omega^2/8)[\mathbf{M}_a]$$

$$- (\lambda(r+2)\Omega/4)([\mathbf{C}_B]+2\Omega[\mathbf{M}_a]) - (\lambda/2)([\mathbf{K}_B]+[\mathbf{K}_a] - \Omega^2[\mathbf{M}_a]))\{b_{r+2}\} = \{0\}, \quad (r = 4, 6, \ldots) \tag{29d}$$

$$(-(r^2\Omega^2/4)[\mathbf{M}_A]+[\mathbf{K}_A])\{b_r\} + (\lambda(r-2)^2\Omega^2/8)[\mathbf{M}_a] + (\lambda(r-2)\Omega/4)([\mathbf{C}_B]+2\Omega[\mathbf{M}_a]) - (\lambda/2)([\mathbf{K}_B]+[\mathbf{K}_a]-\Omega^2[\mathbf{M}_a])\{a_{r-2}\} + (-(\lambda(r+2)^2\Omega/8)[\mathbf{M}_a]) + (\lambda(r+2)\Omega/4)([\mathbf{C}_B]+2\Omega[\mathbf{M}_a]) + (\lambda/2)([\mathbf{K}_B]+[\mathbf{K}_a] - \Omega^2[\mathbf{M}_a])\{a_{r+2}\} = \{0\}, \quad (r = 4, 6, \ldots). \tag{29e}$$

The total amplitude of the periodic solution can be written as

$$A_p = \sum_{k=2,4,6,\ldots}^{N_p} (\{a_k\}^2 + \{b_k\}^2)^{1/2},$$

where N_p is chosen sufficiently large when $\{a_k\}$ and $\{b_k\}$ are sufficiently small and consequently negligible.

4. NUMERICAL RESULTS AND DISCUSSION

The material properties and dimensions of the connecting rod are the same as one of those used by Bahgat and Willmert [13]. Figure 1(a) shows such a slider crank mechanism with the following characteristics: crank length $(OA) = r = 5{\cdot}08 \times 10^{-2}$ m; connecting rod length $(AB) = L = 2{\cdot}54 \times 10^{-1}$ m; crank speed $(\theta_t) = 100{\cdot}0$ rad/s.

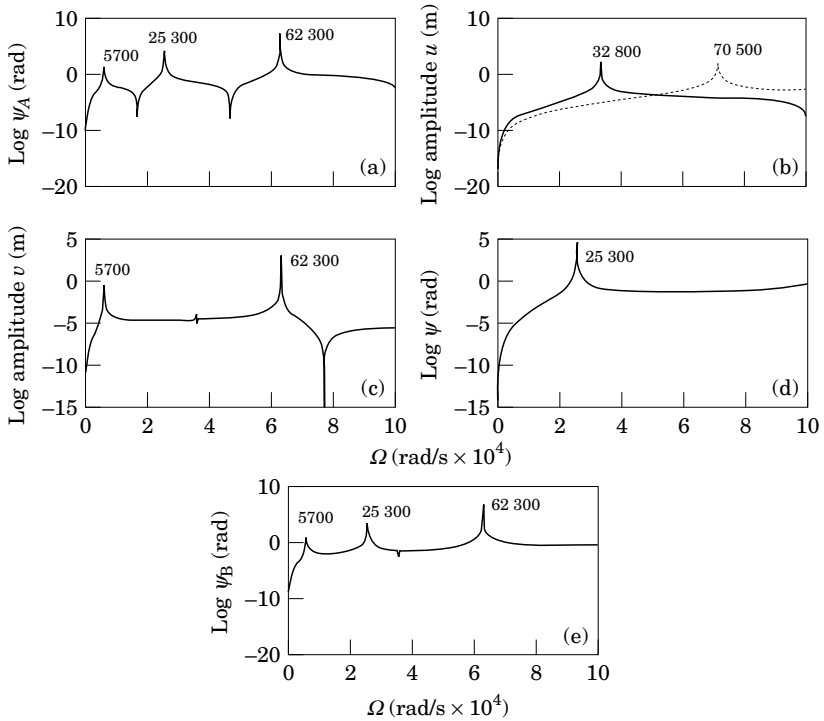

Figure 5. Comparison of the steady-state responses versus crank angular velocity Ω obtained by time-dependent, ——, and simple-supported, - - -, conditions with $\lambda = 0{\cdot}05$. (a) Log ψ_A; (b) Log $(A_p)u$; (c) Log $(A_p)v$; (d) Log ψ; (e) Log ψ_B.

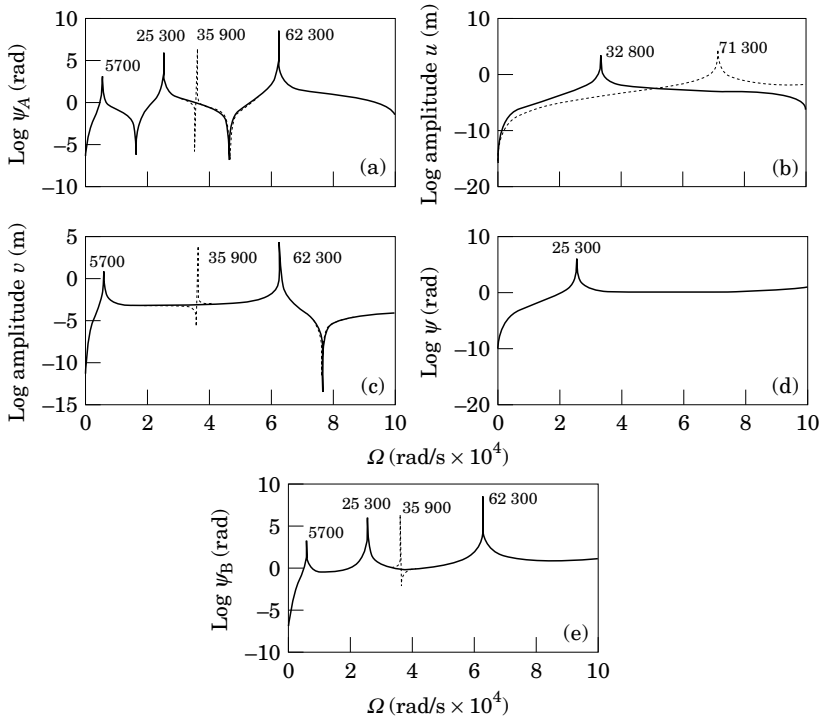

Figure 6. Comparison of the steady-state responses versus crank angular velocity obtained by time-dependent, ——, and simple-supported, - - - , conditions with $\lambda = 0{\cdot}2$ (a) Log ψ_A; (b) Log $(A_p)u$; (c) Log $(A_p)v$; (d) Log ψ; (e) Log ψ_b.

The connecting rod is considered to be a steel rod with modulus of elasticity of $2{\cdot}0684 \times 10^{11}$ N/m^2, mass density of $7{\cdot}74796 \times 10^3$ N s^2/m^4, constant rectangular cross-section $1{\cdot}6129 \times 10^{-4}$ m^2 and Timoshenko shear coefficient $K = 0{\cdot}85$. Here the damping term is taken to be 0.002 times the sum of the mass and stiffness matrix to absorb the amplitudes of high frequency modes.

The constraint conditions (equations 3, 24a, b) of the position, velocity and acceleration obtained in the present paper are different from those obtained by assuming zero displacement, $v_{n+1} = 0$, and utilizing Newton's Second Law to balance the axial, shear loads and inertia force of the piston at $x = L$. Moreover, in the present work the end point B of the connecting rod moves along the X-axis, u_{n+1} and v_{n+1} are not independent, and are related by equation (3). Therefore, the elastic deformation of the end position could be predicted.

On the other hand, it is a second order time-varying periodic differential equation even if the rotation speed Ω is constant. The steady-state solutions of the linear parametric equation can be determined by the harmonic balance method. The dimensionless values of length ratio λ selected in this investigation are 0·2, 0·35, and 0·5. The value of $\lambda = 0{\cdot}5$ was chosen on the basis of the upper limit of the usual slider-crank mechanism design. Four elements are used in the present work. The steady-state amplitudes and rotary angles for various length ratios are shown in Figure 4. It is seen that as the length ratio increases, the steady-state responses also increase. However, the resonant frequencies remain the same. The first mode resonant frequencies of u, v and ψ are 32 800 rad/s, 700 rad/s and 25 300 rad/s, respectively. These values are close to the frequency ($\pi/2L\sqrt{E/\rho} =$ 3195 rad/s) of the fixed-free ends in the u-direction, the frequency ($\pi^2\sqrt{EI/\rho AL^4} =$

5795 rad/s) of the pinned-pinned ends in the v-direction and the frequency ($\pi/L\sqrt{KG/\rho}$ = 36 900 rad/s) of free-free ends in the ψ-direction.

Figures 5a–e give the comparison of the steady-state responses obtained for cases of time-dependent and simply-supported boundary conditions. A length ratio $\lambda = 0{\cdot}05$ is taken. The two sets of results are almost the same, except in the longitudinal direction. In the present paper, the simply-supported condition is replaced by the time-dependent condition. Thus, the frequency decreases from 70 500 rad/s to 32 800 rad/s in the longitudinal direction.

Figures 6a–e show the comparison of the responses for a large length ratio $\lambda = 0{\cdot}2$ between the present work and the simply-supported condition [7, 8]. It is seen that a new natural frequency for the simply-supported condition is excited between the second mode and the third mode frequencies of ψ_A and ψ_B. For this large length ratio the natural frequency in the longitudinal direction increases from 70 500 rad/s (Figure 5(b)) to 71 300 rad/s (Figure 6(b)).

5. CONCLUSIONS

This paper studies the steady-state response of the flexible connecting rod of a slider-crank mechanism. The main point in the present work is that the boundary condition of the connecting rod is a time-dependent boundary support and not a purely simple one. In other words, the simply-supported boundary condition at end point B $V(1, \tau) = 0$ is now replaced by $V(1, \tau) = U(1, \tau) \tan \phi$.

The finite element technique is developed to solve such a problem with time-dependent boundary support. Due to the constant angular velocity of the crank, the equation of motion becomes a time-varying periodic differential equation. The steady-state solution of the linear parametric equation is determined by the harmonic balance method. From the formulation and results obtained, the following conclusions can be drawn:

(1) In the case of the simply-supported end, it is seen that when $u_{n+1} = v_{n+1} = 0$, and there is no deformation at end point B, the piston position of an elastic connecting rod will be the same as that of a rigid body one. Thus, the assumption of the simply-supported end does not contribute to the determination of the end position. However, the elastic deformation of end position could be determined according to the present work.
(2) When the crank length increases, the steady-state responses of u, v, and ψ increase.
(3) The steady-state responses of the time-dependent boundary condition are almost the same as those of the simply-supported condition except in the axial direction.

ACKNOWLEDGMENT

Support of this work by the National Science Council of the Republic of China through Contract NSC 84-2212-E-033-009 is gratefully acknowledged.

REFERENCES

1. P. W. Jasinski, H. C. Lee and G. N. Sandor 1971 *American Society of Mechanical Engineers, Journal Engineering for Industry* **93**, 636–644. Vibrations of an elastic connecting rod of a high-speed slider-crank mechanism.
2. B. V. Viscomi and R. S. Arye 1971 *American Society of Mechanical Engineers, Journal Engineering for Industry* **93**, 251–262. Non-linear dynamic response of an elastic slider-crank mechanism.

3. J. P. Sadler and G. N. Sandor 1973 *American Society of Mechanical Engineers*, *Journal of Engineering for Industry* **95**, 549–557. A lumped parameter approach to vibration and stress analysis of elastic linkages.
4. S. C. Chu and K. C. Pan 1975 *American Society of Mechanical Engineers*, *Journal of Engineering for Industry* **97**, 542–550. Dynamic response of a high speed slider-crank mechanism with an elastic connecting rod.
5. M. Badlani and W. Kleninhenz 1979 *American Society of Mechanical Engineers*, *Journal of Mechanical Design* **101**, 149–153. Dynamic stability of elastic mechanism.
6. M. Badlani and A. Midha 1982 *American Society of Mechanical Engineers*, *Journal of Mechanical Design* **104**, 159–167. Member initial curvature effects on the elastic slider-crank mechanism response.
7. Z. G. Zhu and Y. Chen 1983 *American Society of Mechanical Engineers*, *Journal of Mechanism, Transmissions and Automation in Design* **105**, 637–640. The stability of the motion of a connecting rod.
8. I. G. Tadjbakhsh and C. J. Younis 1986 *American Society of Mechanical Engineers*, *Journal of Mechanism, Transmissions and Automation in Design* **108**, 487–496. Dynamic stability of the flexible connecting rod of a slider crank mechanism.
9. S.-R. Hsieh and S. W. Shaw 1994 *Journal of Sound and Vibration* **170**, 25–49. The dynamic stability and nonlinear resonance of a flexible connecting rod: single-mode model
10. O. P. Agrawal and A. A. Shabana 1985 *Computer & Structures* **21**, 1303–1312. Dynamic analysis of multibody system using component modes.
11. K. Farhang and A. Midha 1991 *Proceedings of the* 13*th ASME Conference on Mechanical Vibration and Noise* **37**, 167–176. Investigation of parametric vibration stability in a slider-crank mechanism with elastic coupler.
12. K. J. Bathe 1982 *Finite element procedures in engineering analysis*. Englewood Cliffs, NJ:Prentice-Hall.
13. B. M. Bahgat and K. D. Willmert 1974 *Mechanism and Machine Theory* **11**, 47–71. Finite element vibrational analysis of planar mechanisms.

APPENDIX A

Details of the shape function are

$$N_{u_1} = 1 - \xi, \qquad N_{u_2} = \xi, \qquad N_{v_1} = [1 - 3\xi^2 + 2\xi^3 + (1 - \xi]/(1 + \Phi),$$

$$N_{v_2} = [\xi - 2\xi^2 + \xi^3 + (\xi - \xi^2)\Phi/2]l/(1 + \Phi), \qquad N_{v_3} = (3\xi^2 - 2\xi^3 + \xi\Phi)/(1 + \Phi),$$

$$N_{v_4} = [-\xi^2 + \xi^3 - (\xi - \xi^2)\Phi/2]l/(1 + \Phi), \qquad N_{\psi_1} = 6(-\xi + \xi^2)/[l(1 + \Phi)],$$

$$N_{\psi_2} = [1 - 4\xi + 3\xi^2 + (1 - \xi)\Phi]/(1 + \Phi), \qquad N_{\psi_3} = 6(\xi - \xi^2)/[l(1 + \xi)],$$

$$N_{\psi_4} = (-2\xi + 3\xi^2 + \xi\Phi)/(1 + \Phi), \qquad \Phi = 12EI/KGAl^2, \quad \xi = x/l.$$

For the kinetic energy (14) of an element:

$$[m_1] = \rho A \int_0^l [N_u^{\mathrm{T}} N_u + N_u^{\mathrm{T}} N_v]\,\mathrm{d}x + \rho I \int_0^l N_\psi^{\mathrm{T}} N_\psi\,\mathrm{d}x,$$

$$[m_2] = \rho A\dot{\phi}^2 \int_0^l [N_u^{\mathrm{T}} N_u + N_v^{\mathrm{T}} N_v]\,\mathrm{d}x + \rho I\dot{\phi}^2 \int_0^l N_\psi^{\mathrm{T}} N_\psi\,\mathrm{d}x,$$

$$[m_c] = \rho A\dot{\phi} \int_0^l [N_v^{\mathrm{T}} N_u - N_u^{\mathrm{T}} N_v]\,\mathrm{d}x,$$

$$[m_{qt}] = -\rho Ar\dot{\theta}\sin(\theta + \phi) \int_0^l N_u\,\mathrm{d}x + \rho A[r\dot{\theta}\cos(\theta + \phi) - \dot{\phi}x_o] \int_0^l N_v\,\mathrm{d}x$$

$$- \rho A\dot{\phi} \int_0^l xN_v \, \mathrm{d}x - \rho I\dot{\phi} \int_0^l N_\psi \, \mathrm{d}x,$$

$$[m_q] = -\rho A[x_0\dot{\phi}^2 - r\dot{\theta}\dot{\phi} \cos(\theta + \phi)] \int_0^l N_u \, \mathrm{d}x + \rho A\dot{\phi}^2 \int_0^l xN_u \, \mathrm{d}x$$

$$- \rho Ar\dot{\theta}\dot{\phi} \sin(\theta + \phi) \int_0^l N_v \, \mathrm{d}x,$$

$$X_1 = \tfrac{1}{2}\rho A[r^2\dot{\theta}^2 - 2r\dot{\theta}\dot{\phi}x_o \cos(\theta + \phi) + \dot{\phi}^2 x_0^2] \int_0^l \mathrm{d}x$$

$$+ \tfrac{1}{2}\rho I\dot{\phi}^2 \int_0^l \mathrm{d}x + \rho A(x_0\dot{\phi}^2 - r\dot{\theta}\dot{\phi} \cos(\theta + \phi)) \int_0^l x \, \mathrm{d}x + \tfrac{1}{2}\rho A\dot{\phi}^2 \int_0^l x^2 \, \mathrm{d}x.$$

For the strain energy (17) of an element:

$$[K_u] = EA \int_0^l [B_u]^{\mathrm{T}}[B_u] \, \mathrm{d}x, \qquad [K_b] = EI \int_0^l [B_b]^{\mathrm{T}}[B_b] \, \mathrm{d}x, \qquad [K_s] = kGA \int_0^l [B_s]^{\mathrm{T}}[B_s] \, \mathrm{d}x.$$

For the kinetic energy (18) of the slider:

$$[m_{41}] = M_4[N_u^{\mathrm{T}}N_u + N_v^{\mathrm{T}}N_v]_{\xi=1}, \qquad [m_{42}] = M_4\dot{\phi}^2[N_u^{\mathrm{T}}N_u + N_v^{\mathrm{T}}N_v]_{\xi+1},$$

$$[m_{43}] = M_4\dot{\phi}^2[N_u^{\mathrm{T}}N_v - N_v^{\mathrm{T}}N_u]_{\xi=1},$$

$$[m_{44}] = \{M_4[L\dot{\phi}^2 - r\dot{\theta}\dot{\phi} \cos(\theta + \phi)]N_u^{\mathrm{T}}\}_{\xi=1} - \{M_4r\dot{\theta}\dot{\phi} \sin(\theta + \phi)N_v^{\mathrm{T}}\}_{\xi=1},$$

$$[m_{45}] = \{M_4[r\dot{\theta} \cos(\theta + \phi) - L\dot{\phi}^2]N_v^{\mathrm{T}}\}_{\xi=1} - \{M_4r\dot{\theta} \sin(\theta + \phi)N_u^{\mathrm{T}}\}_{\xi=1},$$

$$X_2 = \tfrac{1}{2}M_4r^2\dot{\theta}^2 - M_4rL\dot{\theta}\dot{\phi} \cos(\theta + \phi) + \tfrac{1}{2}M_4L^2\dot{\phi}^2.$$

For the work (19) done by the applied force and friction force:

$$[m_w] = \{(F \cos\phi - \mu N \cos\phi - N \sin\phi)N_u^{\mathrm{T}}\}_{\xi=1} + \{(F \sin\phi - \mu N \sin\phi + N \cos\phi)N_v^{\mathrm{T}}\}_{\xi=1},$$

$$X_3 = Fr[\cos\phi \cos(\theta + \phi) + \sin\phi \sin(\theta + \phi)] + Nr[\sin\phi \cos(\theta + \phi) - \cos\phi \sin(\theta + \phi)] + \mu Nr[\cos\phi \cos(\theta + \phi) + \sin\phi \sin(\theta + \phi)] + FL \cos\phi - L\mu N \cos\phi - LN \sin\phi.$$

For the steady-state analysis (25) of a time-varying system:

$$[\mathbf{M}_A]_e = \rho A \int_0^l [N_u^{\mathrm{T}}N_u + N_v^{\mathrm{T}}N_v] \, \mathrm{d}x + \rho I \int_0^l N_\psi^{\mathrm{T}}N_\psi \, \mathrm{d}x,$$

$$[\mathbf{C}_B]_e = \rho A\Omega \int_0^l [N_v^{\mathrm{T}}N_u - N_u^{\mathrm{T}}N_v] \, \mathrm{d}x,$$

$$[\mathbf{K}_A]_e = EA \int_0^l N_{u,x}^{\mathrm{T}} N_{u,x}\, \mathrm{d}x + EI \int_0^l N_{\psi,x}^{\mathrm{T}}\, N_{\psi,x}\, \mathrm{d}x + kGA \int_0^l [N_{v,x} - N_\psi]^{\mathrm{T}} [N_{v,x} - N_\psi]\, \mathrm{d}x,$$

$$[\mathbf{K}_B]_e = \rho A \Omega^2 \int_0^l [N_v^{\mathrm{T}} N_u - N_u^{\mathrm{T}} N_v]\, \mathrm{d}x, \qquad [\mathbf{F}_1]_e = -L\Omega^2 \rho A \int_0^l N_u\, \mathrm{d}x,$$

$$[\mathbf{F}_2]_e = R_0 \Omega^2 \rho A \int_0^l N_v\, \mathrm{d}x - L\Omega^2 \rho A \int_0^l N_v\, \mathrm{d}x + \Omega^2 \rho A \int_0^l x N_v\, \mathrm{d}x + \Omega^2 \rho I \int_0^l N_\psi\, \mathrm{d}x.$$

APPENDIX B

The functions of θ and λ are as follows:

$$\phi = \sin^{-1}(\lambda \sin\theta) = \lambda \sin\theta + \lambda^3 \sin^3\theta/6 + O(\lambda^5),$$

$$\dot{\phi} = \lambda\dot{\theta} \cos\theta/\cos\phi = \lambda\dot{\theta} \cos\theta + \lambda^3\dot{\theta} \sin^3\theta \cos\theta + O(\lambda^5),$$

$$\dot{\phi}^2 = \lambda^2\dot{\theta}^2 \cos^2\theta + O(\lambda^4), \qquad \ddot{\phi} = -\lambda\dot{\theta}^2 \sin\theta + \lambda^3\dot{\theta}^2(\sin\theta \cos^2\theta - 1/2 \sin^3\theta) + O(\lambda^5),$$

$$\sin(\theta + \phi) = \sin\theta + 1/2\lambda \sin 2\theta - 1/2\lambda^2 \sin^3\theta + O(\lambda^4),$$

$$\cos(\theta + \phi) = \cos\theta - \lambda \sin^2\theta - 1/2\lambda^2 \cos\theta \sin^2\theta + O(\lambda^4),$$

$$\sin\phi = \lambda \sin\theta + O(\lambda^3), \quad \cos\phi = 1 + O(\lambda^2), \quad \tan\phi = \lambda \sin\theta, \quad \sec^2\theta = (1/\cos\theta)^2 = 1.$$